OPTOELECTRONICS AND ADVANCED MATERIALS – RAPID COMMUNICATIONS Vol. 3, No. 6, June 2009, p. 553 - 558

Structure and optical constants of electron beam deposited zinc nitride films

H. A. MOHAMED[a]
Physics department, faculty of Science, Sohag University, 82524 Sohag, Egypt
[a]Physics department, Teachers College , King Saud University, 11148 Riyadh, KSA

Zinc nitride (ZnN) films were prepared by electron beam evaporation technique. The effect of heat treatments on the structural and optical properties of these films were studied. The as-deposited films show amorphous structure and some peaks which are related to Zn_3N_2 and ZnO can be observed for annealed films. The study of the optical gap shows that these films have direct optical ban gap about 3.2 eV at temperature 350 ^oC. At high temperature, the ZnN films become more opaque and resistive. Other optical parameters such as refractive index, extinction coefficient and dispersion parameters were investigated as a function of annealing temperature.

(Received May 17, 2009; accepted June 15, 2009)

Keywords: Zinc nitride, Thin films, Electron beam, Optical properties

1. Introduction

Transparent thin-film transistors (TTFTs) is considered one of the new research field of transparent electronics that based on oxide semiconductors [1, 2]. ZnO or ZnO-based compound was used as channel layer of TTFTs. Since then many workers attempted to fabricate TTFTs with improved output characteristics. Most of these reports on TTFTs make use of bottom-gate transistor configuration and as channel material InZnO [3,4], ZnSnO [5], GaSnZnO [6] and InGaZnO [7] has been employed. Recently, Aperathitis et al [8] employed another Zinc compound, for the first time, as a channel layer in TTFTs, namely zinc nitride (ZnN). Though it is n-type material, there is a controversy concerning its optical band gap. The energy gap of this material depends on the deposition technique [9-13] and /or the oxygen impurities [14]. Therefore, the energy gap values have been reported to be between 1.01 eV and 3.2 eV. It was reported that zinc nitride has a direct band gap about 3.2 eV [9, 10] and cubic structure [13]. However, various values and different type of band gap have been obtained. In 2005, Toyoura et al. [11] prepared zinc nitride films using molten salt electrochemical process, and they reported the band gap was 1.01–1.23 eV. In 2006, Zong et al. [13] prepared zinc nitride films on quartz substrates through reactive rf magnetron sputtering, and the films had an indirect band gap of 2.12 eV.

Up to now, although it is expected that zinc nitride will exhibit excellent electrical and optical properties, it has not been finally confirmed whether zinc nitride is a narrow or wide band gap material, and it is also controversial whether its band gap is direct or indirect. Furthermore, the research on the defect and instability of zinc nitride films is needed to continue. More information about its structure and optical constant must be collected to give a deep understanding of theses material and its applications.

In the present study, the electron beam evaporation technique was employed to deposit zinc nitride into glass substrates. The structure and some optical constants such as; transmission, reflection, refractive index, extinction coefficient, energy gap, optical free carrier concentrations, plasma frequency, optical resistivity and dispersion parameters were investigated as a function of annealing temperature.

2. Experimental details

The zinc nitride (ZnN) powder has been made in tablet form using a cold pressing technique. Thin films of the prepared ZnN tablets were deposited onto ultrasonically cleaned glass substrates by electron beam evaporation technique using Edwards high vacuum coating unit model E306A. The deposition process has taken place under conditions of : (1) a vacuum of 3×10^{-5} Torr, (2) an acceleration voltage of 2.5 kV, (3)electron beam current 8-14 mA, and (4) the film thickness (~ 150 nm) and deposition rate (2 Å/s) were controlled by means of a calibrated digital film thickness monitor model TM200 Maxtek. Investigations of the microstructure were carried out using a Phillips PW-1710 Cu-k_α diffractometer (λ = 1.541 838 Å) by varying the diffraction angle 2θ from 4 to 80 by a step width of 0.04 in order to evaluate the crystalline phase and crystallite orientation. A Jasco model

V-570 (UV – VIS – NIR) double beam spectrophotometer was employed to record the transmission T and reflection R over the wavelength range from 200 to 2500 nm at normal incidence with a scan speed of 100 nm/min. The optical measurements were done in the present of reference. The heat treatment (annealing temperature) has been performed in air at different temperatures from 200 to 500 ^{o}C for fixed time of 30 min using a fully controlled furnace (model Lendberag).

3. Results and discussion

The x-ray diffraction (XRD) analysis was performed on as-deposited and annealed zinc nitride films at 350 ^{o}C and the results are shown in Fig. 1. The XRD analysis of the two patterns indicates the ZnN film are amorphous with some small impeded peaks. The peak that locates at $2\theta = 36.79$ implies that the films have a cubic anti-bixbyite of Zn_3N_2 with plane of (400) (JCPDS, card No. 35-0762). A similar results were obtained by Tianlin et al [15]. The other peaks locate at $2\theta = 40.2$, 55.8 are corresponding to ZnO with plane of (002) and (102), respectively. As clearly seen in this figure, the intensity of observed peaks increases with the increasing of annealing temperature up to 350 ^{o}C indicating an enhancement in the carrier mobility of ZnN films [16].

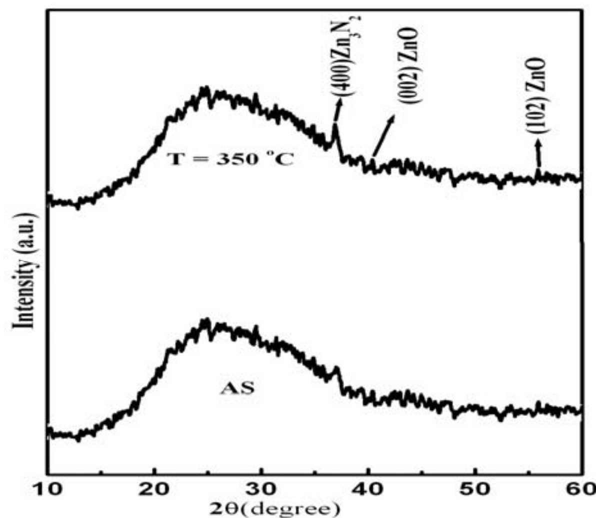

Fig. 1. x-ray diffraction analysis of as-deposited and annealed zinc nitride (ZnN)films at temperature 350°C.

Fig. 2 shows the optical transmission spectra of as-deposited and annealed zinc nitride films at different temperatures (200 – 500 ^{o}C).

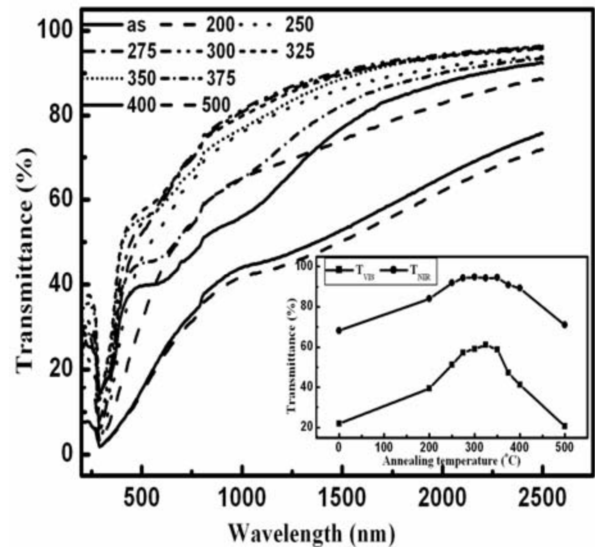

Fig. 2. Transmission spectra of as-deposited and annealed zinc nitride (ZnN)films at different temperatures. In the inset the average transmission in the VIS and NIR regions.

The inset figure shows the average transmission in the visible region (T_{VIS}) and in the near infrared region (T_{NIR}). The as-deposited films have low relatively transmission in both visible (22 %) and near infrared region (69 %). It is noted that, the transmission of annealed films increases with increasing the annealing temperature and attains its maximum value of 62 % and 94% in VIS and NIR regions, respectively at temperature 350 ^{o}C. With further increase in temperature the increase in transmission can be observed and a dramatically decrease can be achieved at temperature 500 ^{o}C, since the transmission records values less than those obtained for as-deposited films. The increase in transmission in the temperature range 0-350 ^{o}C is due to the increase in optical energy gap resulting from the enhancement in the film structure (see Fig. 1). Besides, the increase in transmission may be due to the decrease in free carrier concentration (will be discussed) and hence the decrease in free carrier absorption [17]. According to Walff [18] and Hazem et al [19] at high carrier concentrations, the conduction band is shifted downward and with decreasing the carrier concentration the shift decreases and hence the energy gap increases. Seen in the figure, the absorption edge is shifted to low wavelength (high energy) with increasing the annealing temperature up to 350 ^{o}C and then starts to shift to high wavelength with further increase in temperature. The decrease in transmission at high temperature values may be due to the conversion of the ZnN films from n-type to p-type. Kambilafka et al [20] reported that, the thermal oxidation up to 550 ^{o}C converted all zinc nitride films prepared by r f-sputtering from n-type into p-type materials, exhibiting high resistivity and low carrier concentrations.

Using the measured values of transmission (T) and reflection (R), the absorption coefficient α can be written in the form [16]:

$$\alpha = \frac{2.303}{d} \log_{10}\left(\frac{1-R}{T}\right) \quad (1)$$

where d is the film thickness.

The absorption coefficient can be used to determine the optical band gap E_g according to the following equation:

$$\alpha h\nu = A\left(h\nu - E_g\right)^n \quad (2)$$

where A is a constant, $h\nu$ is the photon energy and the exponent, n=1/2 for allowed direct, n=2 for allowed indirect, n=3/2 for forbidden direct and n=3 for forbidden indirect transitions. In the present study, the zinc nitride films represents direct allowed transitions (n=1/2) and the energy gap was determined by extrapolating the linear portion of the curves to zero absorption as shown in Fig. 3 (a). The obtained energy gap was plotted as a function of annealing temperature and the results are shown in Fig. 3 (b). It can be seen that, the energy gap becomes more wide with increasing the annealing temperature. Since, at 350 ^oC the maximum energy gap value 3.22 eV was obtained. This value is in good agreement with other works [8, 21] and contradicts with the indirect band gap that was reported by other works [13, 15].

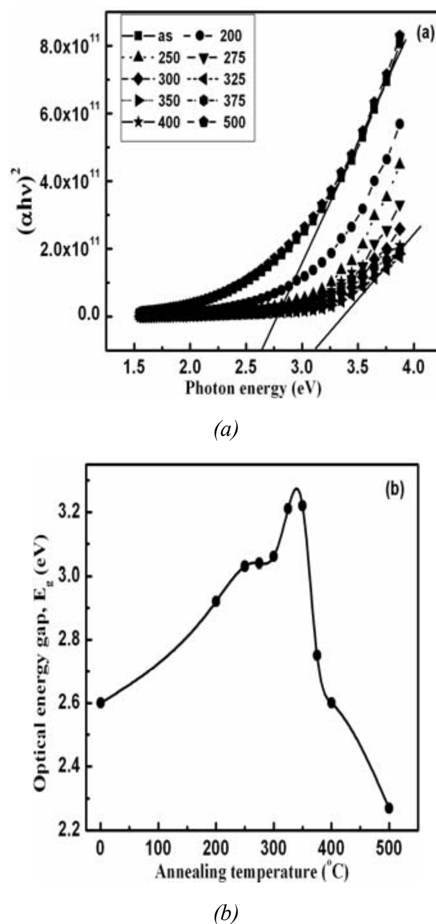

(a)

(b)

Fig. 3. A plot of $(\alpha h\nu)^2$ versus photon energy (a) and the calculated direct optical energy gap (b) of zinc nitride (ZnN)films at different annealing temperatures.

The refractive index n and extinction coefficient k were determined from the reflection and transmission data using the following equations [22]:

$$n = \frac{1+R}{1-R} \pm \left[\left(\frac{R+1}{R-1}\right)^2 - \left(1+k^2\right)\right]^{1/2} \quad (3)$$

$$k = \frac{\alpha\lambda}{4\pi} \quad (4)$$

More reasonable values of refractive index have been obtained using the plus sign of equation 3 in the present work. The average values in the visible region of refractive index and extinction coefficient for as-deposited and annealed zinc nitride films were calculated and plotted in Fig. 4. It is clear that the refractive index decreases with temperature and most samples have refractive index values between 2 and 3, the behavior of refractive index may be due to the decrease in reflection with temperature [23] and/or it can be attributed to the decrease in the packing density [24].

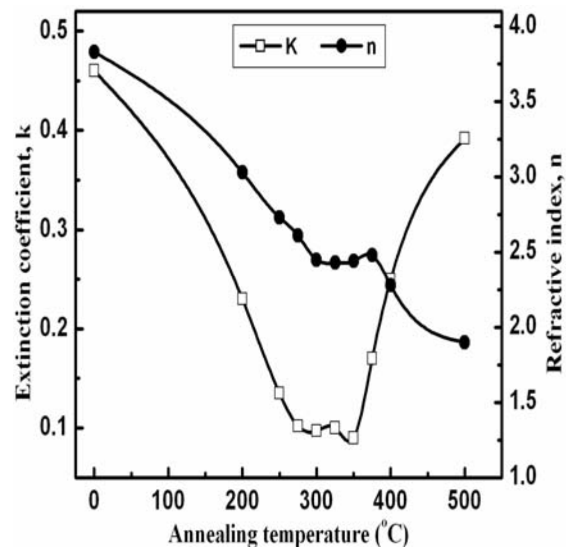

Fig. 4. Plot of refractive index and extinction coefficient of zinc nitride films as a function of annealing temperature.

Fig. 5 represents the typical reflection spectra of as-deposited and annealed ZnN films at different temperatures. The inset figure shows the average reflection in the near infrared region (R_{NIR}). The behavior of reflection with annealing temperature is considered an important tool to understand and then explain the behavior of other optical parameters such as refractive index (see Fig. 4), free carrier concentration and plasma frequency.

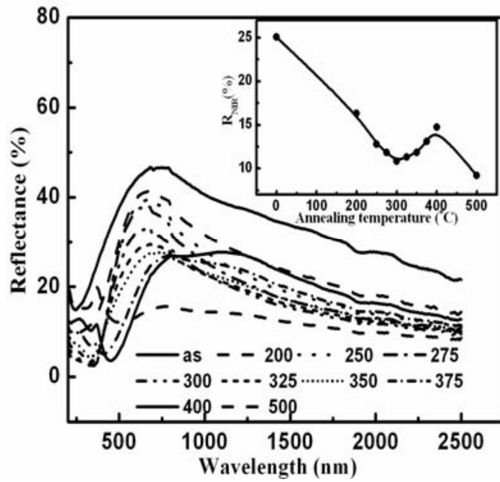

Fig. 5. Reflection spectra of as-deposited and annealed zinc nitride (ZnN)films at different temperatures. In the inset the average reflection in the NIR region.

By using the Drude's theory, the real part of the dielectric function can be written as[25]:

$$\varepsilon^{/} = n^2 - k^2 = \varepsilon_i - \frac{e^2}{4\pi^2 c^2 \varepsilon_0}\left(\frac{N}{m^*}\right)\lambda^2 \quad (5)$$

where ε_i is the infinity high frequency dielectric constant, e is the elementary charge, c is the light velocity, ε_0 is the permittivity of free space, N is the optical free carrier concentration, m^* is the effective mass and λ is the light wavelength. By plotting $\varepsilon^{/}$ versus λ^2 and fitting the straight line as shown in Fig. 6, the free carrier concentration can be determined from the slope. The obtained free carrier concentrations as a function of annealing temperature are shown in Fig. 7.

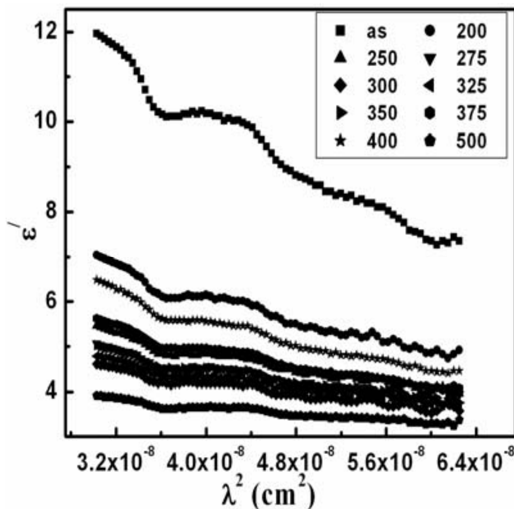

Fig. 6. Plot of a real part of the dielectric constant ($\varepsilon^{/}$) as a function of wavelength for as-deposited and annealed zinc nitride films at different temperatures.

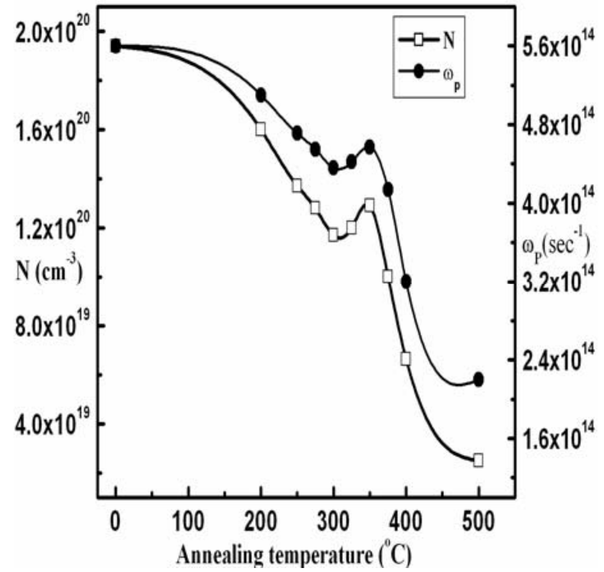

Fig. 7. Variation of the free carrier concentration (N) and plasma frequency (ω_P)with annealing temperature of zinc nitride films.

It is clear that, the carrier concentrations decrease with increasing the annealing temperature up to 350 °C but their values not less than1.3×10^{20} cm^{-3} and this behavior agrees with the behavior of reflection (see Fig. 5). At high temperature a significant decrease in free carrier concentration can be observed. Since at temperature 500 °C, the free carrier concentration record a minimum value of 18×10^{18} cm^{-3}. This may be due to the conversion of the material from n-type to p-type. On the other hand, the plasma frequency ω_P is given by [26]:

$$\omega_P = \left(\frac{N e^2}{\varepsilon_0\, \varepsilon_i\, m^*}\right)^{1/2} \quad (6)$$

As shown in Fig. 7, it is clear that the plasma frequency is directly proportion to the free carrier concentration and this result is in good agreement with Drude's theory.

The dispersion parameters namely; single oscillator energy (E_0) and dispersion energy (E_d) play an essential role in design the optical devices. According to the dispersion theory, the refractive index n is given by [27]:

$$\left(n^2 - 1\right)^{-1} = \frac{E_0}{E_d} - \frac{1}{E_0 E_d}(h\nu)^2 \quad (7)$$

The parameter E_0 is directly related to the optical band gap and E_d is measure of the strength of interbank optical transitions. Fig. 8 represents the variation of E_0 and E_d of zinc nitride films with the annealing temperature. From this figure, it is seen that, the single oscillator energy has the same behavior of the optical energy gap (see Fig. 3-b) and its value is around 1 eV.

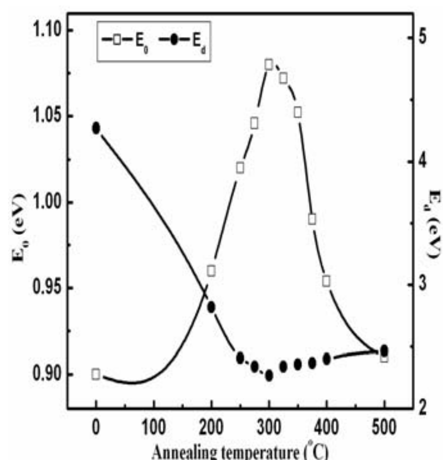

Fig. 8. Plot of a single oscillator energy E_0 and a dispersion energy E_d of zinc nitride films as a function of annealing temperature.

The optical resistivity ρ_{opt} is considered one of the important optical parameters and its behavior agrees with the electrical resistivity [19, 28, 29]. On the other hand, the value of optical resistivity is lower by one order than the electrical resistivity [19]. The optical resistivity is given by:

$$\rho_{opt} = \frac{1}{\varepsilon_i \varepsilon_0 \omega_P^2 \tau} \tag{8}$$

where τ is the relaxation time that can be written in the form [30]:

$$\varepsilon^{//} = 2nk = \frac{\varepsilon_i \omega_P^2}{4\pi^3 c^3 \tau} \lambda^3 \tag{9}$$

where $\varepsilon^{//}$ is the imaginary part of the dielectric constant.

Fig. 9 shows the variation of optical resistivity with annealing temperature of zinc nitride films.

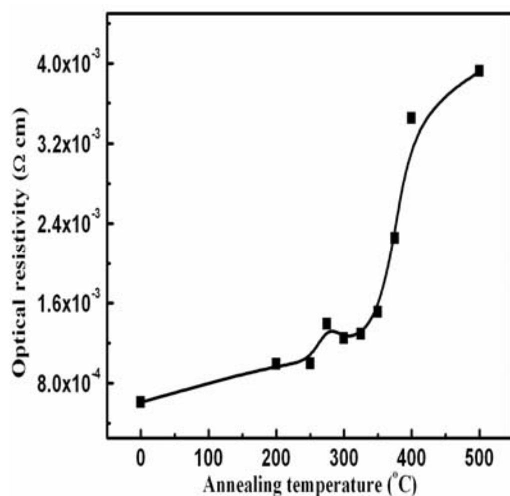

Fig. 9. Variation of the optical resistivity with annealing temperature of zinc nitride films.

It is clear that, the as-deposited films are conductive material. The resistivity of as-deposited films are about 6 $\times 10^{-4}$ (Ω cm). With increasing the temperature of annealing , the films become more resistive since the resistivity records 3.45×10^{-3} (Ω cm) at temperature 500 °C. The increase of optical resistivity with annealing temperature is due to the decrease of the optical free carrier concentration as shown in Fig. 7.

4. Conclusions

Zinc nitride is considered one of the new materials that have many applications in transparent electronics. In the present study, the electron beam method was used to prepare zinc nitride films. It was concluded that:

1) The as-deposited films exhibit amorphous structure and the crystallinity is weakly improved with temperature.

2) The films have direct allowed band gap of 3.2 eV at temperature 350°C. And this band gap records a minimum value of 2.25 eV at temperature 500 °C.

3) The optical constant such as refractive index, extinction coefficient, carrier concentration, plasma frequency, oscillation energy, and dispersion energy are more sensitive to the annealing temperature.

4) At high temperature, the ZnN films represent low transmission (~ 20%), low free carrier concentrations (18×10^{18} cm^{-3}), and low conductivity (3.45×10^{-3} Ω cm). This behavior is may be due to the conversion of the ZnN material from n-type to p-type.

Acknowledgements

I am grateful to Dr. T. Taha for his cooperation and help in preparing the zinc nitride powder.

References

[1] K. Nomura, H. Ohta, K. Ueda, T. Kamiya, M. Hirano, H. Hosono, Science **300,** 1269 (2003).
[2] J. F. Wager, Science **300**, 1245 (2003).
[3] D. C. Paine, B. Yaglioglu, Z. Beiley, S. Lee, Thin Solid Films **516**, 5894 (2008).
[4] R. Martins, P. Barquinha, I. Ferreira, L. Pereira, G. Goncalves, E. Fortunato, J. Appl. Phys. **101**, 044505 (2007).
[5] D. Hong, H. Q. Chiang, F. G. Wager, J. Vac. Sci. Technol. B**24**, L23 (2006).
[6] R. Martins, Presented at the 2nd International Symposium on Transparent Conductive Oxides (ISTCO), Crete, Greece, Oct. 21–24, 2008.
[7] H. Kumoni, K. Nomura, T. Kamiya, H. Hosono, Thin Solid Films **516**, 1516 (2008).
[8] E. Aperathitis, V. Kambilafka, M. Modreanu, Thin Solid Films, in press, 2009.
[9] K. Kuriyama, Y. Takahashi, F. Sunohara, Phys. Rev. B **48,** 2781 (1993).

[10] M. Futsuhara, K. Yoshioka, O. Takai, Thin Solid Films **322**, 274 (1998).
[11] K. Toyoura, H. Tsujimura, T. Goto, K. Hachiya, R. Hagiwara, Y. Ito, Thin Solid Films **492**, 88 (2005).
[12] W. Du, F. Zong, H. Ma, J. Ma, M. Zhang, X. Feng, H. Li, Z. Zhang, P. Zhao, Cryst. Res. Technol. **41**, 889 (2006).
[13] F. Zong, H. Ma,W. Du, J. Ma, X. Zhang, H. Xiao, F. Ji, C. Xue, Appl. Surf. Sci. **252**, 7983 (2006).
[14] T. Suda, K. Kakishita, J. Appl. Phys. **99**, 076101-1 (2006).
[15] T. Yang, Z. Zhang, Y. Li, M. Lv, S. Song, Z. Wu, J. Yan, S. Han, Applied Surface Science **255**, 3544 (2009).
[16] H. A. Mohamed, J. Phys. D: Appl. Phys. **40,** 4234 (2007).
[17] H. Kim, J. Horwitz, W. Kim, A. Makinen, Z. Kafafi, D. Chrisey, Thin Solid Films **420–421**, 539 (2002).
[18] P. Wolff, Phys. Rev. **126**, 405 (1962).
[19] H. M. Ali, H. A. Mohamed, M. M. Wakkad, M. F. Hasaneen, Thin Solid Films **515**, 3024 (2007).
[20] V. Kambilafka, P. Voulgaropoulou, S. Dounisb, E. Iliopoulos, M. Androulidaki, V. S. Aly, M. Ruzinsky, E. Aperathitis, Superlattices and Microstructures **42**, 55 (2007).
[21] V. Kambilafka, P. Voulgaropoulou, S. Dounis, E. Iliopoulos, M. Androulidaki, K. Tsagaraki, V. Šály, M. Ružinský, P. Prokein, E. Aperathitis, Thin Solid Films **515**, 8573 (2007).
[22] J. Tauc, in: J. Tauc (Ed.), Amorphous and Liquid Semiconductors, Plenum Press, New York, 159, 1979.
[23] P. P. Sahay, S. Tewari, R. K. Nath, Cryst. Res. Technol. **42**, 723 (2007).
[24] H. A. Mohamed, H. M. Ali, Sci. Technol. Adv. Mater. **9,** 025016 (2008).
[25] C. H. L. Weijtens, P. A. C. Van loon, Thin Solid Films**196**, 1(1991).
[26] I. Saadeddin , B. Pecquenard , J. P. Manaud , R. Decourta, C. Labruge`re ,T. Buffeteau, G. Campet, Applied Surface Science **253**, 5240 (2007).
[27] F. Yakuphanoglu, A. Cukurovali, I. Yilmaz, Physica B **353,** 210 (2004).
[28] H. Haitjema, J. J. Ph. Elich, Thin Solid Films **205**, 93 (1991).
[29] J. Ederth, P. Hezler, A. Hulatåker, G. A. Niklasson, C. G. Granqvist, Thin Solid Films **445**, 199 (2003).
[30] H. A. Mohameda, H. M. Ali, S. H. Mohamed, M. M. Abd El-Raheem, Eur. Phys. J. Appl. Phys. **34**, 7 (2006).

*Corresponding author: hussein_abdelhafez2000@yahoo.com